metals

MDPI

Article

Influence of Material and Process Parameters on Reduction-Swelling Characteristics of Sintered Iron Pellets

Kedarnath Rane [1,*], Prashant Date [2] and T. S. Srivatsan [3]

[1] Advanced Forming Research Centre, National Manufacturing Institute Scotland, Renfrewshire PA4 9LJ, UK
[2] Department of Mechanical Engineering, Indian Institute of Technology Bombay [IIT B], Mumbai 400076, India
[3] Department of Mechanical Engineering, The University of Akron, Akron, OH 44325, USA
* Correspondence: kedarnath.rane@strath.ac.uk

Abstract: This paper investigates the use of shop-floor ferrous scrap that contains iron ore as a raw material for the purpose of making steel products through an in situ carbothermic reduction. The technique of powder metallurgy (PM) was used for the purpose of studying reduction followed by densification during sintering. Two sources of iron oxide—ferrous grinding-sludge powder and iron ore—and three sources of the carbonaceous material—graphite, charcoal, and carbon black—were considered. The carbonaceous material was added to the iron oxide after calculating the stoichiometric carbon requirement for facilitating both direct reduction and direct–indirect reduction. This involves a simultaneous change in weight and volume. During sintering, an in situ reduction of the iron oxide takes place that often results in severe volumetric changes. The test results revealed the degree of reduction (DOR) and degree of densification (DOD) of the grinding sludge (GS) to be 15% and 45% higher, respectively, than that of iron ore (IO). This is essentially due to the presence of distinct iron-oxide phases coupled with a greater amenability to the occurrence of carbothermic reduction. Indirect reduction also took place and contributed to improving the degree of reduction (DOR) and degree of densification (DOD) of the final products. Overall, the shape stability of the sintered grinding-sludge (GS) powder was found to be optimized when parameter settings of graphite (from 25% in excess to 50% in excess) were added, a compaction pressure of 1050 MPa was applied, and a sintering temperature of 1200 °C was employed. Hence, ferrous scrap can be chosen as direct reduced iron for the manufacture of steel and can also be used for cost-efficient and eco-friendly structural components with a marginal compromise on both the purity and strength of the ferrous products.

Keywords: carbothermic reaction; sintering; swelling; reduction; densification

Citation: Rane, K.; Date, P.; Srivatsan, T.S. Influence of Material and Process Parameters on Reduction-Swelling Characteristics of Sintered Iron Pellets. *Metals* **2023**, *13*, 141. https://doi.org/10.3390/met13010141

Academic Editor: Francisco Paula Gómez Cuevas

Received: 3 November 2022
Revised: 12 December 2022
Accepted: 14 December 2022
Published: 10 January 2023

1. Introduction

Ferrous metal scrap, such as the powdered oxides of iron oxides, are receptive to recycling using the powder metallurgy (PM) technique. Recent developments have shown that an in situ reduction of iron oxides is possible and occurs during sintering prior to densification [1]. This is true if the sintering is performed in a reducing atmosphere, such as hydrogen (H_2), carbon monoxide (CO), or methane gas (CH_4) [2,3]. Another cost-effective method for densification is carbothermic reduction, wherein a carbonaceous source is mixed with iron oxide in adequate proportions prior to compaction in order to facilitate the occurrence of an in situ reduction during sintering [4–7]. This type of recycling is best-suited to metallic scrap that is available in a powdered form or that can be transformed into powder. If the new scrap—such as chips, scales, and machining swarf—are oxides of iron, then pulverization is easy due to its intrinsic brittleness. Studies performed elsewhere on the pulverization of metallic scrap have reported success at obtaining powder using a combination of various milling and grinding techniques [8–13].

The powders obtained following the ball milling, target jet milling, or high energy ball milling of scrap metal chips are often irregular in shape [14]. Upon compaction of the

powders, the resultant compact—referred to as the "green" compact—has a higher strength due to the mechanical interlocking of the irregularly shaped powder particles [9,15,16]. Samples sintered in a reducing atmosphere, such as hydrogen (H_2) gas, possess a combination of improved sintered density and mechanical properties [17–20]. This technique has been reported for the recycling of ultra-high-strength steels, low-carbon steel, alloy steels, and even cast iron. Metallic scrap powders obtained from the pulverization of mill scales and chips have also been studied using carbothermic reduction. The source of the reducing agent is either a solid carbonaceous material (such as charcoal, coke or char fines), or gases (such as carbon monoxide or methane) [21,22]. The overall purity and activity of carbon in carbonaceous materials determines the success of the carbothermic reduction route [23,24].

In the present study, the carbothermic reduction technique was used for the purpose of recycling shop floor metallic waste to facilitate both a comparison and reduction of iron ores, which represents the traditional method for making iron. The initial studies revealed that forging scales do not have the potential for solid-state recycling [1,25]. In contrast, downgraded grinding sludge (GS)/swarf was found to show great promise for the purpose of manufacturing a sintered product through the solid-state recycling route [26].

Iron ore is the primary source of iron for making steel. Currently, iron and steel plants have a separate sintering unit for enabling the partial reduction of iron oxide from the iron ore to enable an overall improvement in energy efficiency and resulting in the production of steel [11,27]. These units are used to obtain sinters (partially-reduced iron), which are then used as raw materials in both the iron- and steel-melting furnaces [28–30]. The sintering operation is quite like the sintering stage in the powder metallurgy (PM) process. However, the sintering operation in the powder metallurgy (PM) process also helps in densifying the particulate matter to the desired shape. The iron ore contains stable iron-oxide phases along with traces of non-metallic impurities (such as the oxides of other metals). The iron-oxide phases present in both the grinding sludge (GS) and iron ore (IO) are quite different. However, both can be reduced through the carbothermic reaction [13,31]. This is the point of commonality that is being systematically explored by using two completely different compositions of the powders coming from different sources.

This comparison will also shed light on how the mechanism of reduction varies based on a different combination of phases of iron oxide. Furthermore, one can easily establish the mode of reduction for the different phases of the iron oxide. Experiments were planned using the Taguchi experimental design technique and laid out as an L27 experimental array. The observed weight and volume changes of the pellets after sintering were used for the calculation of the three quality characteristics, namely the following:

(a) The degree of reduction (DOR).
(b) The degree of densification (DOD).
(c) The reduction swelling Index (RSI).

These parameters are defined below. The effect of the experimental parameters and their influence on the quality characteristics is also presented and briefly discussed. The influence of optimal levels of (i) mixing, (ii) reduction in temperature, (ii) use of a reducing agent, and (iv) sintering atmosphere were also studied and established.

2. Material Details

2.1. Grinding Sludge (GS) Powder

The ferrous metal scrap generated during the shop-floor grinding of micro-alloyed steel (chemical composition: 4.37 C, 18.16 O, 0.21 Al, 0.87 Si, 1.02 Mn (weight percent), balance Fe) is referred to as the grinding sludge (GS). The grinding sludge (GS) is dried to remove water and subsequently roasted for the purpose of converting the organic non-metallic constituents such as filter-paper residues and lubricating-oil residues into carbon, which would then be utilized for enabling a carbothermic reaction [1].

After the pulverization of the dried and roasted grinding sludge, it was characterized for both chemical properties and physical properties. The iron-oxide phases present in the grinding sludge demonstrated a dominance of the Fe_3O_4 phase, which is referred

to as Magnetite (Table 1). The Fe_2O_3 phase, which was dominant in the iron ore (IO) powder, was found to be absent in the grinding sludge (GS). The particle size, shape, and surface area were characterized using the Microtrac S3500 SIA apparatus. Approximately 20 mg (milligrams) of either powder sample was dispersed in 20 mL of methanol and then sonicated for full 5 min in a 60 Watts sonicator bath. Two samples each from the grinding-sludge (1 and 2) and iron-ore (1 and 2) powder were used for the measurement of particle size, particle shape, and surface area. The results for particle size and surface area are provided in Table 2. Figure 1 shows that segmented and unevenly distributed shapes of grining sludge whereas iron ore powder is finer and also having uneven distribution. The average aspect ratio of the grinding-sludge powder was found to be 0.55 (Figure 2), while that of the iron-ore powder was essentially an irregular particle shape (Figure 1).

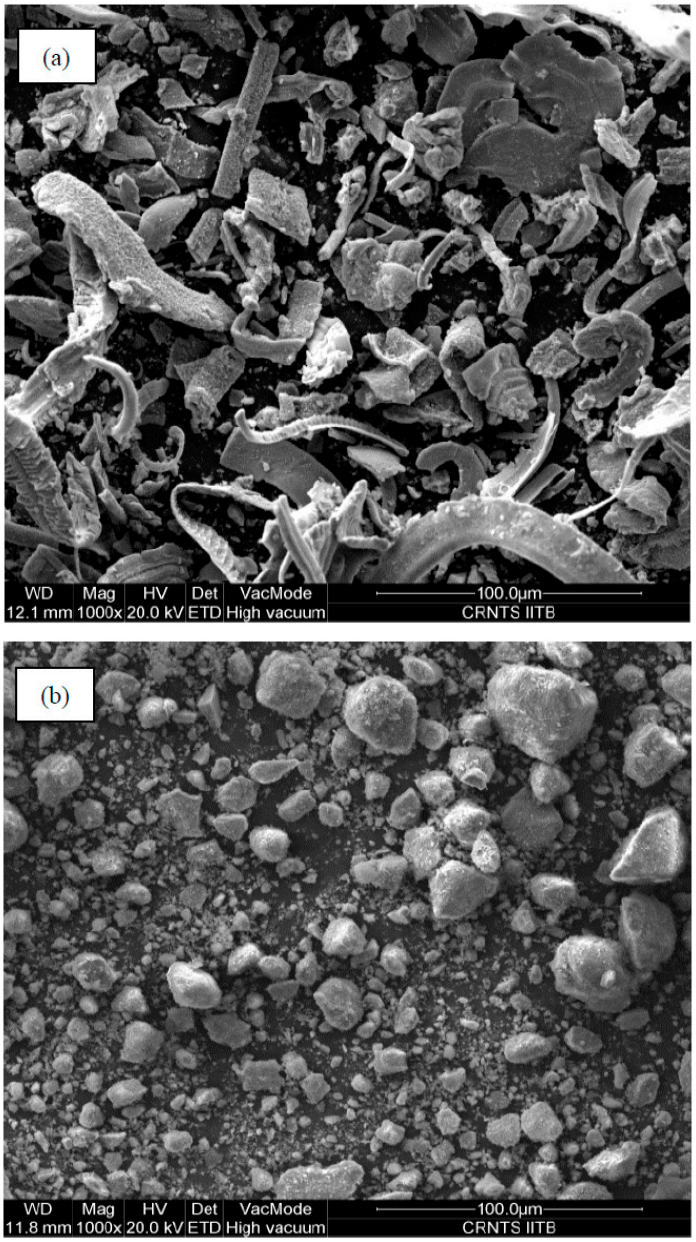

Figure 1. Scanning electron micrographs of (**a**) grinding-sludge powder and (**b**) iron-ore powder.

Table 1. Phase distribution in iron oxide source material.

Material	Constituents %					
	Fe_{Total}	Fe_2O_3	Fe_3O_4	FeO	$Fe_{Metallic}$	Impurity/ Non-Metallic
Grinding Sludge (GS)	75.72	Nil	92.78	1.92	1.44	Nil
Iron Ore (IO)	59.77	84.21	Nil	0.70	Nil	1.73 CaO, 0.24 MgO, 6.56 SiO_2, 5.28 Al_2O_3, 0.16 MnO, 0.31 TiO_2, 0.051NiO_2, 0.08 P_2O_5

Table 2. Average particle size and surface area of iron oxide source material.

	GS Powder		IO Powder	
	Grinding Sludge 1	Grinding Sludge 2	Iron Ore 1	Iron Ore 2
Average particle size (μm)	21.77	29.19	22.62	18.59
Surface Area (m^2/g)	7.87	7.95	8.52	8.76

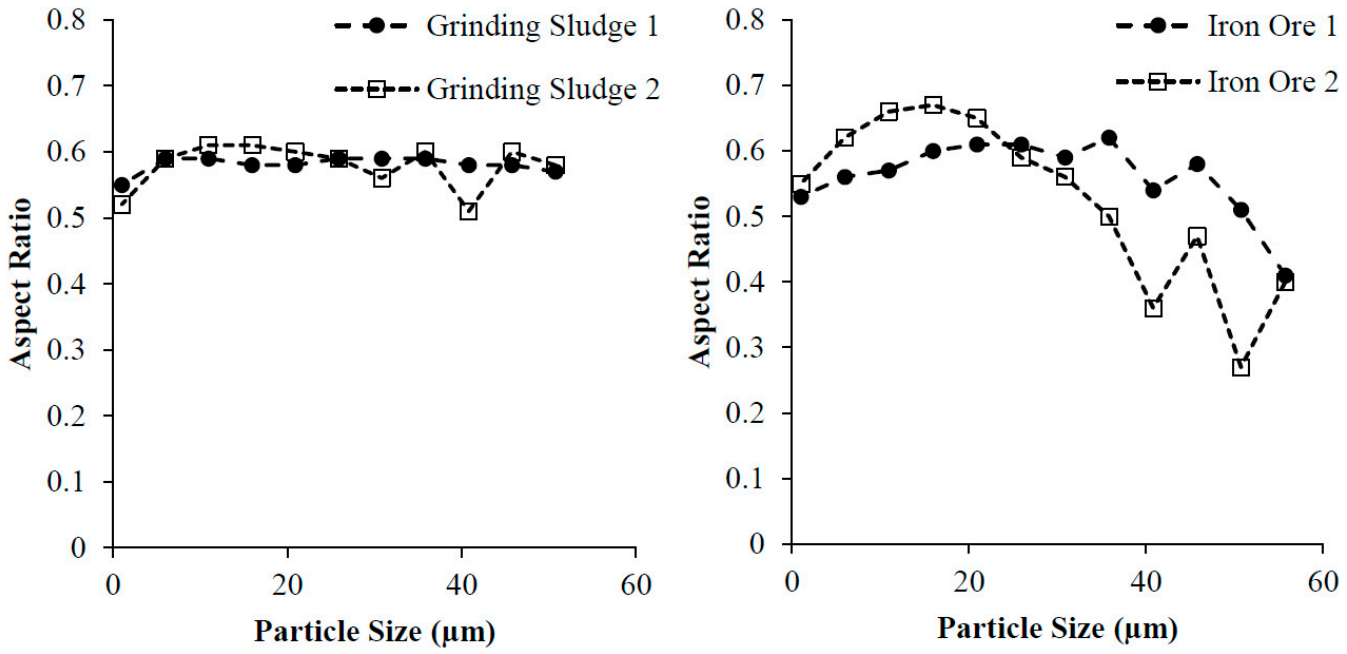

Figure 2. Varying aspect ratio of the powder particles with particle size.

2.2. Iron Ore (IO) Powder

Indian iron ore (obtained from SESA Goa Limited) was first crushed and subsequently pulverized in a ball mill. It was then sieved to obtain the desired particle size (<45 μm). The characteristics of the powdered iron ore, such as (i) iron-oxide phases, (ii) impurities, (iii) particle size, and (iv) surface area, are summarized in Tables 1 and 2. The average particle size of the iron-ore powder was 22.62 and 18.59 μm as tested and averaged from two powder samples. The particle size and shape analysis were conducted using the Microtrac S3500 SIA apparatus in a manner similar to that for the grinding-sludge (GS) powder. The

shape analysis revealed a greater variation in aspect ratio and thereby particle shape with a particle size for the iron-ore (IO) powder than for the grinding-sludge (GS) powder.

2.3. Reducing Agents

The three carbonaceous materials selected for the reduction study include the following: (i) graphite, (ii) carbon black, and (iii) charcoal. The graphite powder (Make: SD Fine Chem.)was procured. Graphite is the purest form of carbon and is available in the flaky form. The charcoal was prepared from wood sawdust using the pyrolysis technique at 600 °C in a laboratory-scale reactor. The carbon-black powder was obtained following pyrolysis of rubber-crumb waste at 600 °C using a laboratory-scale vacuum reactor. The three reducing agents were then sieved through a 325 mesh (44 µm) sieve. The powdered reducing agents were characterized using the proximate analysis. Moisture content in the three chosen reducing agents was precision-measured using procedures detailed in the ASTM D1509-95 Standard. The measurement required heating the material to 125 °C in an oven for 1 full hour and determining the moisture content on the basis of weight loss. Volatile matter (%) was measured in accordance with procedures detailed in the ASTM D3175-11 Standard. This required heating the material to 950 °C for 7 min. The subsequent the loss in weight is a measure of the volatile matter (percent). The ash content was measured in accordance with procedures detailed in the ASTM D3174-11 Standard. The source material was heated to 950 °C for 1 h to allow for a complete burning of the carbon source such that the remaining material was ash. The presence of fixed carbon was determined using the ASTM D3172-07 Standard. A proximate analysis of the chosen reducing agents is given in Table 3. The elemental distribution in each reducing agent was obtained using the CHNSO analysis (with the aid of a device used for the rapid determination of carbon, hydrogen, nitrogen, and sulphur in the materials), which determines the presence of organic constituents (weight percent) in a sample of the reducing agent. The chosen sample was heated to 900 °C and the gases formed during burning were carefully analyzed in a Gas Chromatography attachment. The relative percentages were subsequently determined. Elemental constituents of the reducing agents are tabulated in Table 4.

Table 3. Proximate analysis of reducing agents.

Reducing Agents	Moisture (%)	Volatile Matter (%)	Ash (%)	Fixed Carbon (%)
Graphite	0.67	00.18	01.34	97.81
Charcoal	1.21	21.66	09.86	67.27
Carbon Black	3.20	07.66	09.06	80.08

Table 4. Elemental constituents (percent) of reducing agents from CHNSO analysis.

Elements (%)	Graphite	Charcoal	Carbon Black
C	33.102	66.383	39.714
H	5.589	2.006	9.792
N	2.441	0.328	2.513
O	0.637	6.563	2.838

Fixed carbon is the solid, combustible residue that remains after a carbon source is heated and the presence of any and all volatile matter is expelled. The fixed carbon amount in graphite was the highest, demonstrating negligible amounts of moisture, volatile matter, and ash content. Carbon-black powder contained 80.08% fixed carbon whereas charcoal powder contained 67.27% fixed carbon. The charcoal powder contained 66.383% elemental carbon, which was a higher amount than that of the graphite powder and carbon-black powder. Although graphite had a higher fixed-carbon content than the carbon-black

powder and charcoal powder, the form and overall reduction affinity of both carbon black and charcoal were noticeably higher. Thus, in the present study, the selected reducing agents (charcoal and carbon black) provided a higher degree of reduction and thereby a better combination of mechanical properties.

A sample calculation of the theoretical requirement of carbon for the reduction of 1 g of the grinding-sludge (GS) powder and iron-ore (IO) powder is provided as follows:

(A) The grinding-sludge powder [92.78% Fe_3O_4, 1.92% FeO, 1.44% Fe Metallic, and 3.84% C]

Mechanism 1: Direct–indirect reduction (C=>CO=>CO_2)

$$2Fe_3O_4\ (0.9278)^{\#} + C\ 0.0247 = 6\ FeO\ [0.864]^{*} + CO_2\ 0.088 \quad (1)$$

$$FeO\ (0.0192) + [0.864] + C\ 0.0738 = Fe\ [0.692] + CO_2\ 0.272 \quad (2)$$

$^{\#}$( ) Represents mass obtained from source; *[ ] represents mass obtained from reaction.

$C_{required}$ = 0.0247 + 0.0738 = 0.0985

Mechanism 2: Direct reduction (C=>CO)

$$Fe_3O_4\ (0.9278) + C\ 0.04812 = 3\ FeO\ [0.8636] + CO\ 0.1122 \quad (3)$$

$$FeO\ (0.0192) + [0.864] + C\ 0.1474 = Fe\ [0.6920] + CO\ 0.3437 \quad (4)$$

$C_{required}$ = 0.04812 + 0.1474 = 0.1955

(B) Iron-ore powder [84.21% Fe_2O_3, 0.7% FeO, other oxides, and impurities including Al_2O_3 and SiO_2]

Mechanism 1: Direct–indirect reduction (C=>CO=>CO_2)

$$2\ Fe_2O_3\ (0.8421) + C\ 0.01055 = 4\ Fe_3O_4\ [0.8139] + CO_2\ 0.0386 \quad (5)$$

$$2\ Fe_3O_4\ [0.8139] + C\ 0.0211 = 6\ FeO\ [0.7577] + CO_2\ 0.07735 \quad (6)$$

$$2FeO\ [0.7577] + (0.007) + C\ 0.06392 = 2\ Fe\ [0.594] + CO_2\ 0.2242 \quad (7)$$

$C_{required}$ = 0.01055 + 0.02111 + 0.06392 = 0.09492

Mechanism 2: Direct reduction (C=>CO)

$$Fe_2O_3\ (0.8421) + C\ 0.02111 = 2\ Fe_3O_4\ [0.8139] + CO\ 0.04923 \quad (8)$$

$$Fe_3O_4\ [0.8139] + C\ 0.0422 = 3\ FeO\ [0.7577] + CO\ 0.0984 \quad (9)$$

$$FeO\ [0.7577] + (0.007) + C\ 0.1278 = Fe\ [0.5944] + CO\ 0.2981 \quad (10)$$

$C_{required}$ = 0.02111 + 0.0422 + 0.1278 = 0.1911

3. Design of Experiments Using the Taguchi Technique

The present problem regarding recycling using the powder metallurgy (PM) route requires a careful analysis of the following parameters: (i) mixing technique, (ii) addition of a reducing agent (%), (iii) reduction temperature, (iv) reducing agent, (v) compaction pressure, (vi) sintering condition, and (vii) sintering temperature for process optimization by reduction to obtain good mechanical properties. The seven selected parameters for this present study are neatly tabulated with their respective three levels (Table 5). Among the possible interactions, three parameters—namely, (i) mixing technique, (ii) addition of reducing agents (%), and (iii) reduction in temperature—were chosen for studying their effect and/or influence on the following:

(a) The degree of reduction (DOR).
(b) The degree of densification (DOD).
(c) Mechanical properties.

Table 5. Control parameters with their respective levels used in the study.

Sr. No.	Control Parameters	Levels		
		1	**2**	**3**
1	A: Mixing Technique	Ball Milling	Mixer Grinding	Turbula Mixing
2	B: Reducing Agent Addition (%)	Stoichiometric	25% excess	50% excess
3	C: Reduction Temperature (°C) Below Sintering Temperature	200	100	0
4	D: Reducing Agent	Graphite	Carbon Black	Charcoal
5	E: Compaction Pressure (MPa)	900	1050	1200
6	F: Sintering Condition	Vacuum	Ar	N_2
7	G: Sintering Temperature (°C)	1100	1200	1300

Each parameter has three levels and their outcomes have a linear relationship. The degree of freedom (DOF) was calculated as follows:

$$[(\text{main parameters } 07 \times (3 - 1) = 14) + (\text{interactions } 03 \times 4 = 12)] = 26.$$

The most suitable orthogonal array for the present study is an L27 because it also has 26 degrees of freedom (DOFs) [11–13]. Thus, in order to study the effect of the control parameters summarized in Table 5, a total of 27 runs needed to be conducted.

In the L27 experimental array, 13 columns were available for assigning control parameters and their interactions.

(a) Column numbers 1, 2, 5, 9, 10, 12, and 13 were used for the following: (i) mixing technique, (ii) addition of reducing agent (%),(iii) reduction in temperature, (iv) type of reducing agent, (v) compaction pressure, (vi) sintering condition (atmosphere), and (vii) sintering temperature, respectively.
(b) Column 3 and Column 4 were used to calculate the interaction between the mixing technique and the reducing agent (%).
(c) Column 6 and Column 7 were used for an interaction between the mixing technique and reduction temperature, and
(d) Column 8 and Column 11 were used for studying the interaction between the addition of a reducing agent (%) and the reduction in temperature [19,20].

Powders from the two sources were mixed with different proportions of the reducing agent. The compacted samples were made to study the objectives listed below.

1. To study the mechanisms of reduction; direct–indirect reduction (C=>CO=>CO_2) and direct reduction (C=>CO).
2. To eliminate the effect of noise arising from the batch of powder (namely, different particle sizes).
3. To eliminate effect of noise arising from positioning of the samples in the furnace.

To accommodate all the considered objectives, a total of eight samples needed to be prepared for each experimental condition and for each of the materials chosen and studied, i.e., grinding sludge and iron ore. Thus, a total of 2 × L27 arrays were planned for the study. The L27 experimental array with three levels of factors is provided in Appendix A. The outcome of the 2 × L27 experiments will be useful for a comparative study of both the reduction and densification of the different sources of iron-oxide powder.

4. Experimental Details

In the present experimental study, a calculated amount (stoichiometric; 25% excess and 50% excess) of the reducing agents, such as graphite, carbon black, and charcoal, was carefully mixed using either of the mixing methods detailed below (Figure 3).

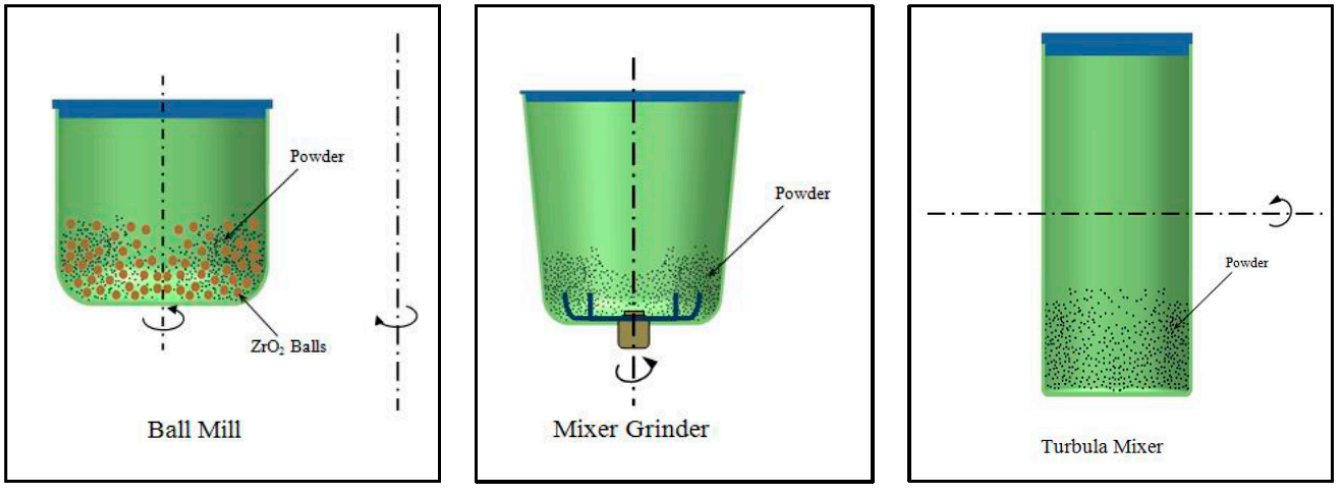

Figure 3. The mixing techniques followed for mixing powdered iron oxides with the reducing agents.

Ball Milling. Scrap powder and a calculated amount of reducing agent were added to the zirconium oxide (ZrO_2) container of a laboratory-scale planetary ball mill in order to maintain a ball–powder ratio of 5:1. The sample was then mixed for 2 × five minutes at 100 rpm. The selection of ball–powder ratio, speed of revolution [i.e., r p m] and mixing time were primarily selected for mixing the two constituents together and not to lower the particle size.

Mixer Grinder. A commercial household mixer appliance was used for the purpose of mixing. The scrap powder and a calculated amount of reducing agent were mixed for a total of 10 min over 5 cycles of 2 min on with 5 min off. The purpose of this process was to restrict a rise in temperature and prevent the erosion of the blades during mixing.

Turbula Mixing. A specially designed and fabricated turbula mixer was also used for the purpose of mixing. The reducing agent and scrap powder were first added to a glass bottle. The glass bottle was then inserted into a rubber cover. This assembly was inserted into a container to ensure proper cushioning of the bottle when the container was rotated to facilitate mixing. The container was rotated at a constant speed of 30 rpm for a full 10 min. There was no pause during the turbula mixing, primarily because this technique allows for mixing without a rise in the temperature.

For every experiment in the L27 array, a total of four powder mixtures were prepared and two samples were prepared from each mixture. This is shown in Figure 4. Thus, for an experiment, 08 samples were used for sintering. Therefore, a total of 432 samples were sintered using 54 sintering cycles [02 sources of iron oxide × L27 experiments × 08 samples per experiments = 432 samples].

The mixtures of iron oxide and the powders of the reducing agent were compacted using a hydraulic press. The die used for compaction was capable of producing cylindrical pellets with a diameter of 10 mm. To begin, all the dies and punches were generously lubricated using a mixture of stearic acid and acetone for the purpose of reducing friction during compaction. For each sample, 2 g of powder mixture was precision-weighed and filled in the die cavity. The powder mixture was then compacted at room temperature (25 °C) using different compaction pressures ranging from 900 MPa to 1200 MPa and without the addition of any binder. A dwell time of 2 min was provided at the end of the stroke. A compaction pressure in the range 600 MPa to 900 MPa, along with a 2 percent polyvinyl glycol binder and a dwell time of 2 min, was used for the compaction of a mixture of iron-ore powder and reducing agent. A change in the range of compaction pressure and binder addition was required for the mixture of iron-ore powder and reducing agent primarily because a layered structure tended to form in the compact with the occurrence of fine microscopic cracking when compacted at pressures beyond 900 MPa.

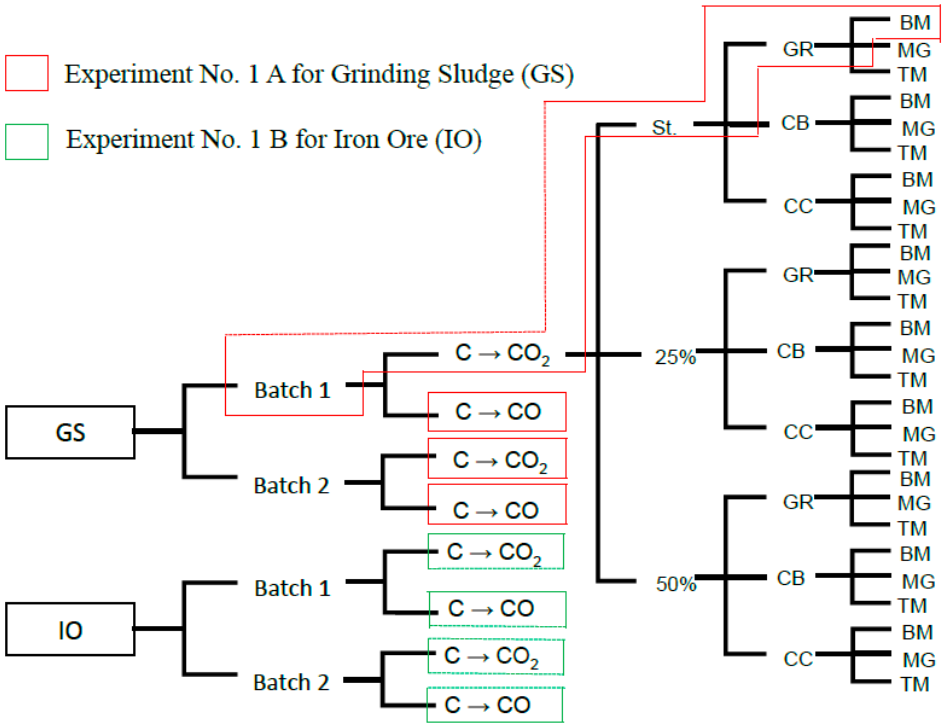

Figure 4. Tree diagram for the mixing of iron oxide and the carbonaceous material.

The compacted samples (referred to as the "green" samples) were subsequently sintered at different temperatures and sintering atmospheres. The reduction in temperatures was set at 200 °C, 100 °C, and 0 °C lower than the sintering temperature. Sintering of the chosen samples was performed in the following environments: (i) vacuum, (ii) argon (Ar) gas, and (iii) nitrogen (N_2) gas. A schematic representation of the sintering arrangement is shown in Figure 5.

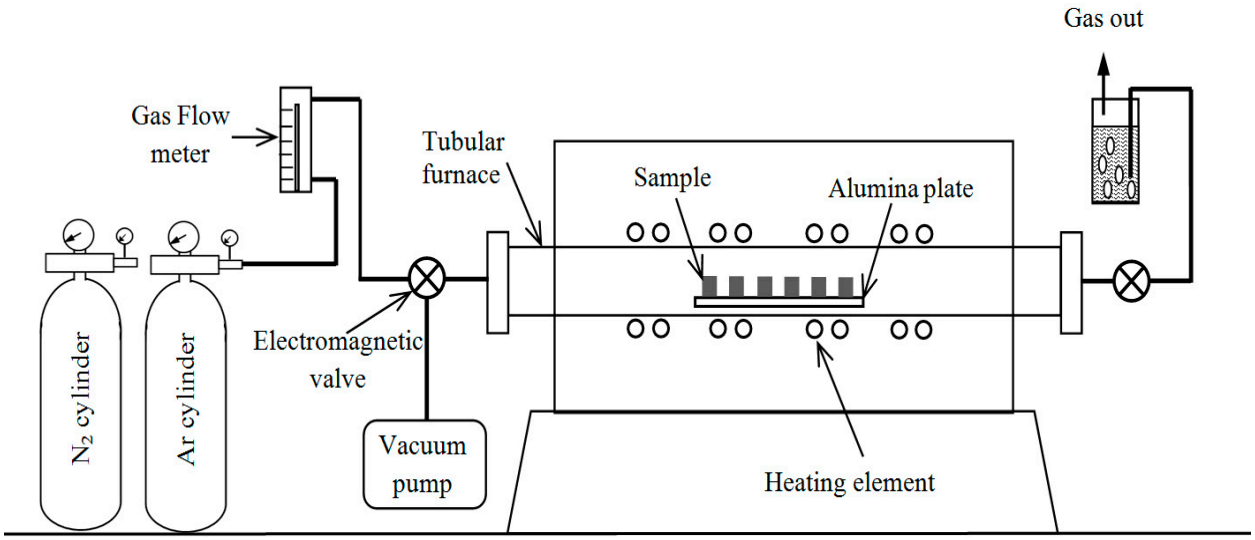

Figure 5. Schematic representation of the sintering furnace used with operating arrangement.

Given that the sintering cycle for an experimental run involves different reduction temperatures (for full 30 min) and sintering temperatures (for 60 min), there were essentially nine types of sintering cycles (as is shown in Figure 6) that were required for sintering in order to complete the L27 experimental array. The arrangement of samples, positioned carefully on an alumina plate for sintering, is shown in Figure 7.

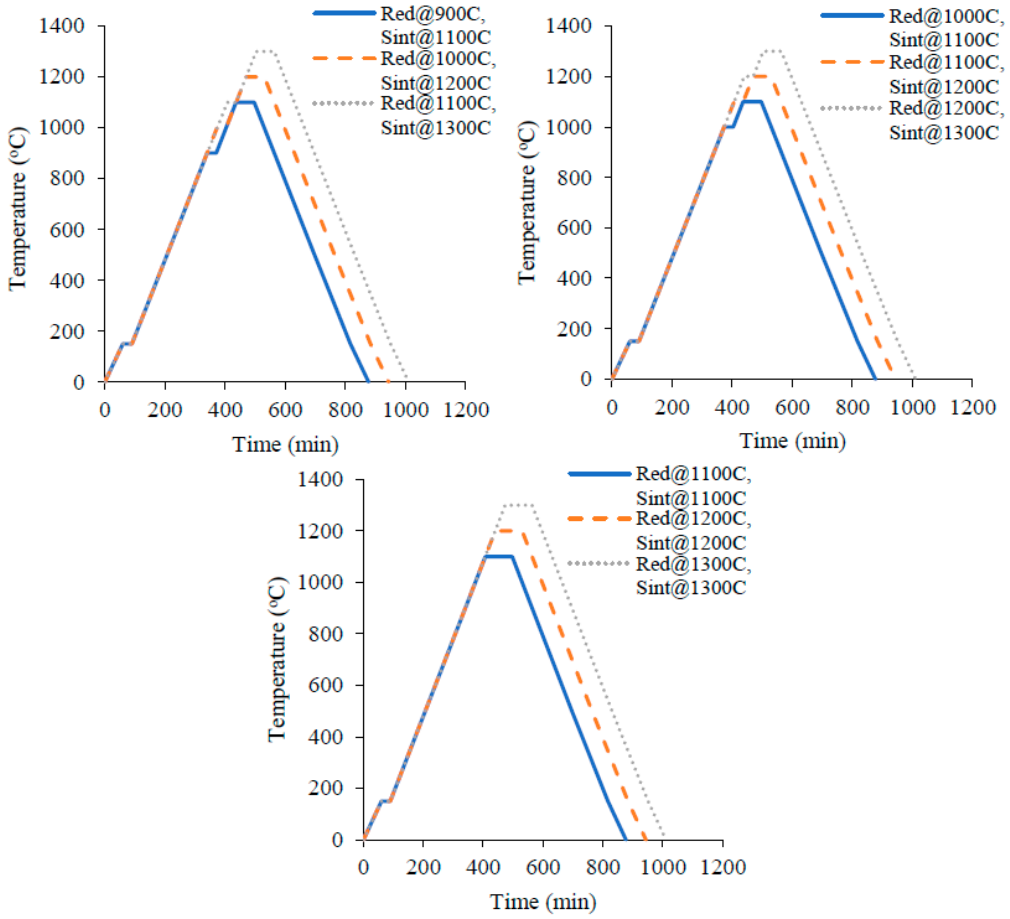

Figure 6. Sintering cycles for different reduction and sintering temperatures.

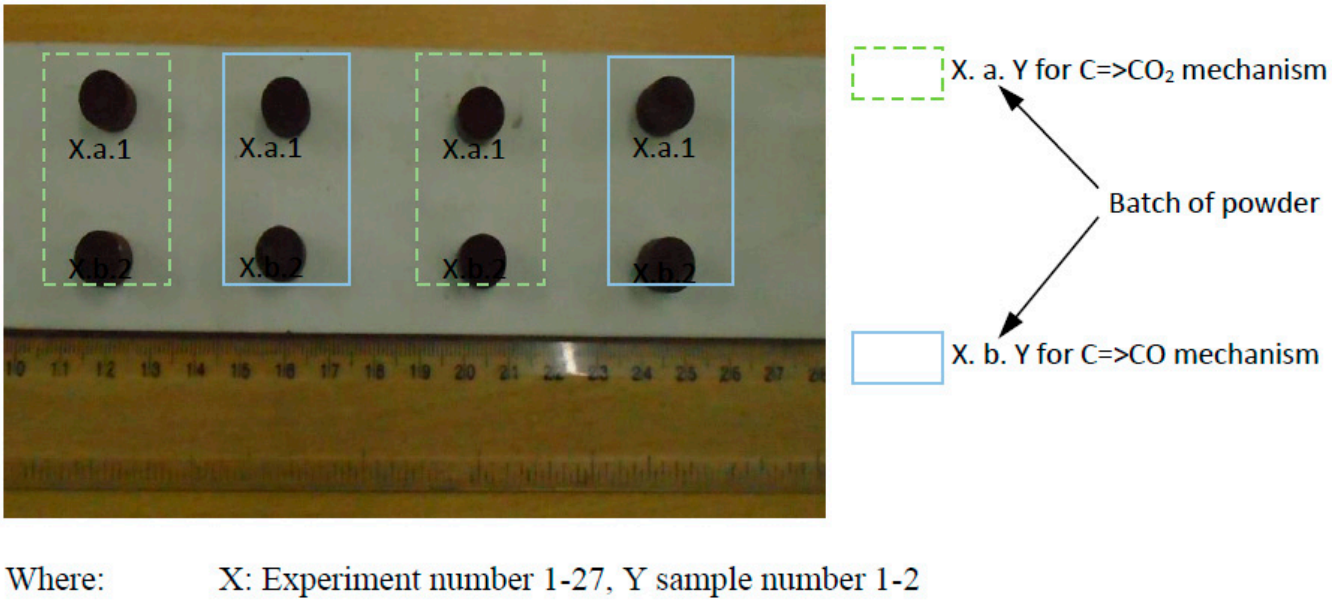

Figure 7. Sample position on an alumina plate while sintering.

For each experiment, eight samples were prepared for both the grinding sludge (GS) and iron ore (IO). Four of these samples were prepared for studying the intricacies specific to the C=>CO=>CO_2 mechanism, while the other four samples were prepared for studying the intricacies specific to the C=>CO mechanism. Among the four samples, two samples

were prepared from a batch of iron-oxide (IO) powder while the other two were replicas of the previous samples. The initial ("green") weight and final (sintered) weight of the samples were precision-measured using a weighing balance with an accuracy of 0.01 g. Similarly, the apparent volumes of both the "green" sample and the sintered sample were determined after the desired dimensions were measured using a vernier caliper having 0.01 mm precision.

5. Results and Discussion

5.1. Degree of Reduction and Degree of Densification

The measured weight and volume of the pellet both before sintering and after sintering were used for enabling the calculation of the degree of reduction (DOR) and the degree of densification (DOD). The formulae used for calculating the degree of reduction (DOR) and degree of densification (DOD) are in accordance with procedures detailed in the ISO 7215:2015 Standard (Expression (11) and Expression (12)).

$$\begin{aligned} \text{Degree of Reduction (DOR)} &= \left(\frac{\text{Actual weight change}}{\text{Theoretical weight change}}\right) \times 100\% \\ &= \left(\frac{\text{Initial weight} - \text{Final weight of sample}}{\text{Initial weight} - \text{Theoretical reduced weight}}\right) \times 100\% \end{aligned} \quad (11)$$

$$\text{Degree of Densification (DOD)} = \left(\frac{\rho_{\text{Sintered}} - \rho_{\text{Green}}}{\rho_{\text{Iron}} - \rho_{\text{Green}}}\right) \times 100\% \quad (12)$$

The calculated DOR and DOD for the L27 experiments were used as "quality" characteristics for the purpose of studying both reduction and densification. The Taguchi analysis technique was used to determine the conjoint influence of material and process parameters used in the current L27 array. To that end, the S/N ratio was calculated for the responses (i.e., quality characteristics) for each of the experiments. A "the larger the better" criterion was applied to interpret the S/N ratio.

The effects of the seven parameters on the degree of reduction (DOR) and degree of densification (DOD) were systematically determined. The main effects and/or influence of these parameters are discussed in the following section.

The effects of mixing technique and quantity of reducing agent on the degree of reduction (DOR) and degree of densification (DOD) are shown in Figure 8. Mixing the grinding sludge using a Turbula mixer or mixer grinder along with a reducing agent for a full 10 min did reveal an insignificant variation in the degree of reduction (DOR) and degree of densification (DOD) (Figure 8a). Upon increasing the quantity of reducing agent (proportional to C for the C=>CO=>CO_2 mechanism and the C=>CO mechanism), as is shown in Figure 8b, the degree of reduction (DOR) increased with an increase in the quantity of the reducing agent. This is due to a noticeable increase in the number of sites for reduction. An insignificant effect on the degree of densification (DOD) due to the mixing technique as well as the quantity of the reducing agent added can be observed from Figure 8b.

A significant upper shift for the degree of densification (DOD) corresponding to the added reducing agent for the purpose of enabling the C=>CO=>CO_2 mechanism of reduction is easily observed in the main-effect plots of the chosen parameters. The key reason for the observed improvement is provided. The reducing agent added for the purpose of the C=>CO reduction was not fully transformed into CO and CO_2. The high proportion of reducing-agent addition in the form of pellets did not allow for the densification to occur due to the limited contact between the transformed metallic iron phases and the residue of the unused carbon. This also placed a hinderance on the stepwise transformation of the iron-oxide phases (Fe_2O_3=>Fe_3O_4=> FeO=>Fe) by indirect reduction. A kinetically efficient indirect reduction was not possible due to the limited exposure of the carbon monoxide (CO) gas to the iron oxide particles caused by residual carbon. The incomplete transformation clearly explains the presence of intermediate iron-oxide phases in the pellets subsequent to sintering. This incomplete transformation decreased the anticipated amount of volume shrinkage and densification subsequent to sintering. In contrast, the carbon that

was added to the pellet for the purpose of the C=>CO=>CO_2 reduction was better utilized, resulting in an overall higher metallic transformation and concomitant improved degree of densification (DOD). A representative scanning electron micrograph (SEM) (Figure 9) revealed the metallic transformation with a porous microstructure.

The added carbothermic reducing agent in different proportions to facilitate an in situ reduction of one gram of grinding-sludge powder is provided in Table 6. The amount of reducing agent in the mixture of iron oxide and reducing agent did increase with both excess addition and mechanism of reduction. An addition of up to 50% in excess of the stoichiometric requirement of the reducing agents (0.1477 g for 1 g of grinding sludge (GS)) gave a higher degree of reduction. However, beyond that, the excess added carbon left behind after sintering resulted in less change in weight during in situ reduction or the resultant lower degree of reduction. The degree of densification (DOD) was influenced by the combined and mutually interactive influences of the respective degree of reduction (DOR) and process parameter settings [1]. Further, the degree of densification (DOD) was less influenced by the addition of a reducing agent. This behavior is well-correlated with the formation and presence of a porous microstructure subsequent to sintering (Figure 9).

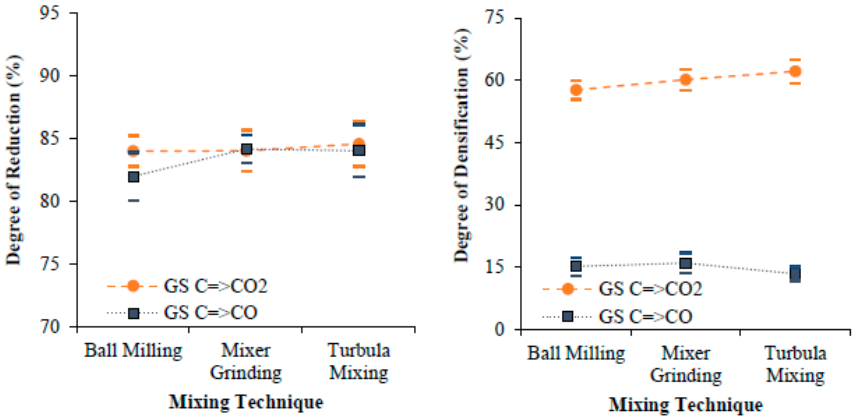

(a) Effect of mixing technique on Degree of Reduction (DOR), and Degree of Densification (DOD)

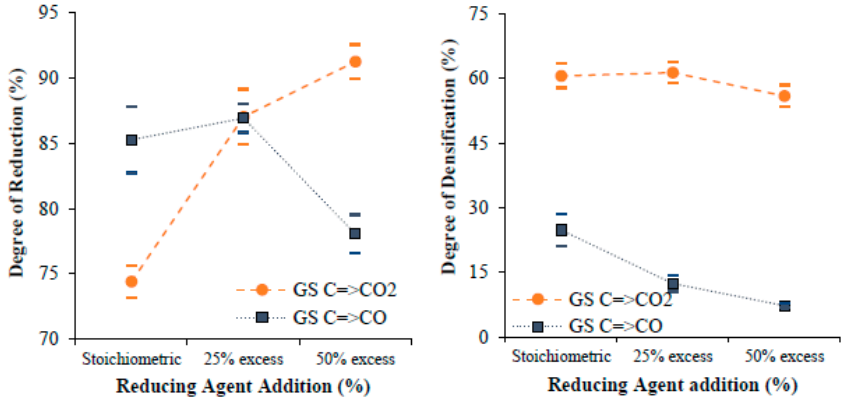

(b) Effect of reducing agent addition on Degree of Reduction (DOR) and Degree of Densification (DOD)

Figure 8. The main effects of (**a**) mixing technique and (**b**) the addition of reducing agent on the degree of reduction (DOR) and degree of densification (DOD) for the grinding sludge.

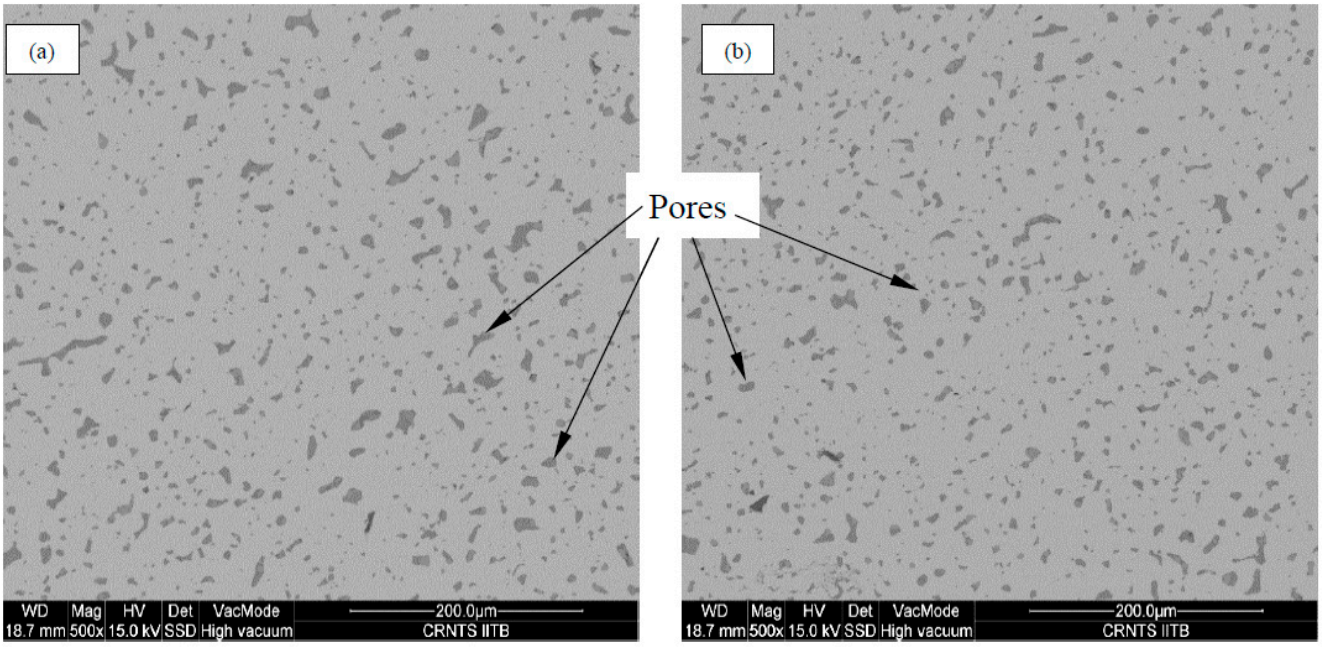

Figure 9. Scanning electron micrograph of the polished surface of sintered samples. Pores in image (**a**) sample from Experiment 22 are larger and more unevenly distributed than in image (**b**) of the sample from Experiment 14.

Table 6. Amount of carbon added to iron oxide for carbothermic reducing.

Proportion of C Addition	Mechanism 1 Direct-Indirect; C=>CO=>CO_2			Mechanism 2 Direct; C=>CO		
	Stoic.	**25% Excess**	**50% Excess**	**Stoic.**	**25% Excess**	**50% Excess**
for Grinding Sludge	0.0985	0.0123	0.1477	0.1955	0.2443	0.2932
for Iron Ore	0.0949	0.1186	0.1423	0.1911	0.2388	0.2866

The reducing agents selected for the present study did not significantly affect or influence the selected characteristics. Both graphite and charcoal did provide an overall better-quality characteristic than carbon black, due to their purity coupled with activity for carbothermic reduction. A reduction in temperature that is 100 °C lower than the sintering temperature is desirable for an improvement in the degree of reduction (DOR). Increasing the temperature of reduction improves the carbothermic reduction reaction. However, too high of a temperature (being the same as the sintering temperature) does lower the degree of reduction (DOR) due to densification. The densification starts immediately after reduction and does not allow for further direct reaction and indirect reaction to occur. A reduction in temperature by 100 °C lower than the sintering temperature also improved the degree of densification (DOD). This was due to a higher fraction of reduced iron as a result of the higher DOR shown in Figure 10a, which allowed for better closure of the fine microscopic pores that are formed after reduction. The sintering atmosphere changed from vacuum to inert gas (argon (Ar) or nitrogen (N_2)), and the inert-gas flow was found to be useful for an improvement of both the DOR and DOD because the useful carbon monoxide (CO) gas (for enabling indirect reduction) would evacuate faster, meaning that CO gas was not present to enable the occurrence of an indirect reduction in the sample. An inert-gas flow at 150 mL/min in the furnace tube is comparatively lowered to help in the evacuation of gases which contribute to the occurrence of indirect reduction. Thus, the degree of reduction (DOR) and degree of densification (DOD) are noticeably improved for the case of an inert-gas atmosphere (Figure 10b All figures should be cited in sequential order). An increase in the sintering temperature revealed a considerable increase in both

the degree of reduction (DOR) and degree of densification (DOD) up until 1200 °C, but remained unchanged thereafter. This is shown in Figure 10c. A combination of reduction in temperature of 1100 °C and a sintering temperature of 1200 °C provided for a high degree of reduction (DOR). However, the degree of densification (DOD) continued to increase from 1200 °C to 1300 °C due to the occurrence of the diffusion-controlled mechanism that caused pore shrinkage during sintering [5,17].

A change in compaction pressure from 900 MPa to 1200 MPa did not significantly influence and/or alter both the reduction and densification characteristics. However, a 1050 MPa compaction pressure was found to result in a noticeably higher degree of reduction (DOR) and degree of densification (DOD). The effect of material and process parameters on both the DOR and DOD of iron ore were similar to that of the grinding sludge (GS). However, the DOR and DOD of the iron ore (IO) sample were significantly lower than that of the grinding sludge (GS) sample due to the presence of Fe_2O_3 phases and impurities.

Among the interaction effects, most of the interaction showed a synergetic interaction between the mixing technique and a reduction in temperature (Figure 11a,b) on both the degree of reduction (DOR) and degree of densification (DOD), while the addition of a reducing agent and reduction in temperature revealed no interaction.

Between the selected parameters for the two key characteristics considered, i.e., the DOR and DOD, a combination of mixer-grinding technique and the addition of 25% excess reducing agent did contribute to enhancing reduction and densification. Similarly, a combination of the mixer-grinding technique for mixing and a reduction of 100 °C below the sintering temperature did reveal a high degree of densification. The mixing technique did show a significant variation in both the degree of reduction (DOR) and degree of densification (DOD), with the turbula mixing being a better mixing technique for an overall improvement of the quality characteristics of iron ore, as is shown in Figure 12a. The suitability of turbula mixing for the mixing of iron ore and the reducing agent is obvious given that the particles of iron (whiskers of irregular size) are mixed well with the reducing agent by way of low-energy mixing. An addition of the reducing agent in 50% excess of the stoichiometric requirement for reduction did reveal an observably higher degree of reduction (DOR), while a 25% excess of the stoichiometric requirement did provide a higher degree of densification (DOD) for the reduction mechanism of C=>CO=>CO_2. This is shown in Figure 12b.

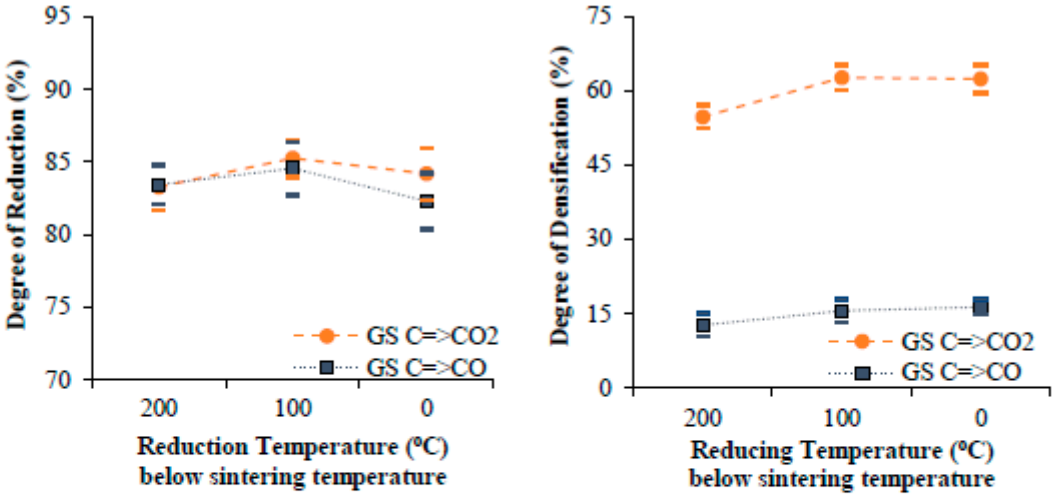

(a) Effect of Reduction Temperature on Degree of Reduction (DOR) and Degree of Densification (DOD)

Figure 10. *Cont.*

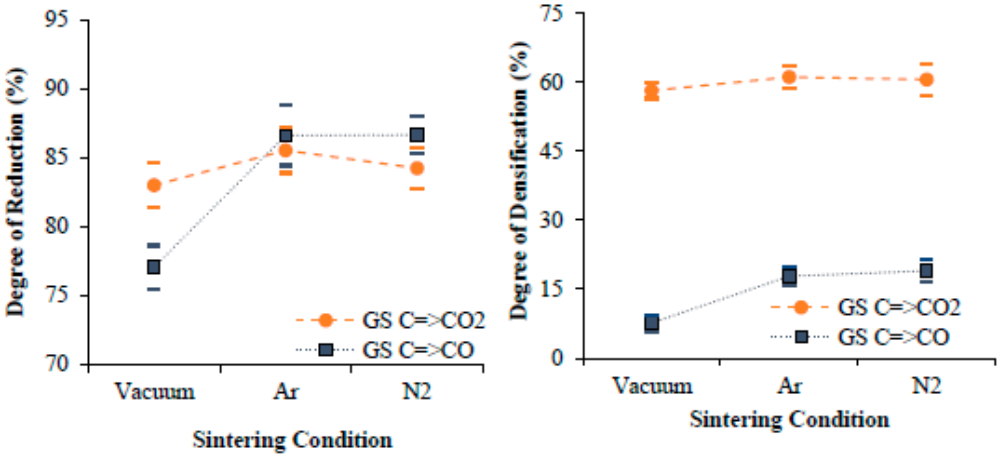

(b) Effect of sintering condition/atmosphere on Degree of Reduction (DOR) and Degree of Densification (DOD)

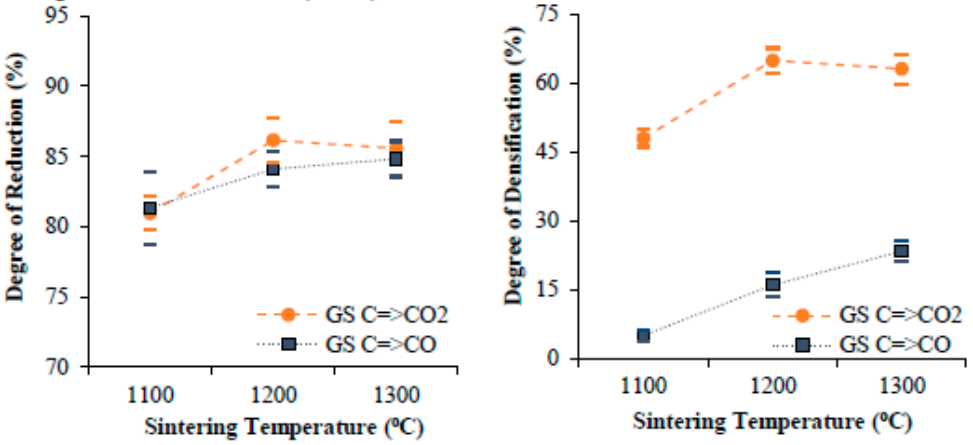

(c) Effect of Sintering Temperature on Degree of Reduction and Degree of Densification

Figure 10. Main effects on the degree of reduction and degree of densification of grinding sludge: of (**a**) reduction in temperature, (**b**) sintering condition or atmosphere, and (**c**) sintering temperature.

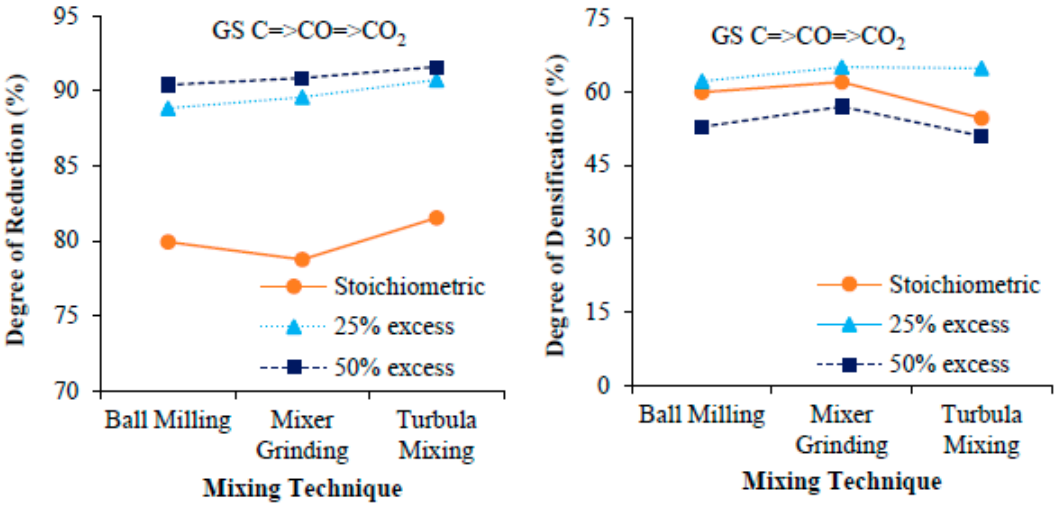

(a) Effect of interaction between Mixing Technique and Reducing agent addition on Degree of Reduction (DOR) and Degree of Densification (DOD) characteristics for the C => CO => CO_2 reduction mechanism.

Figure 11. *Cont.*

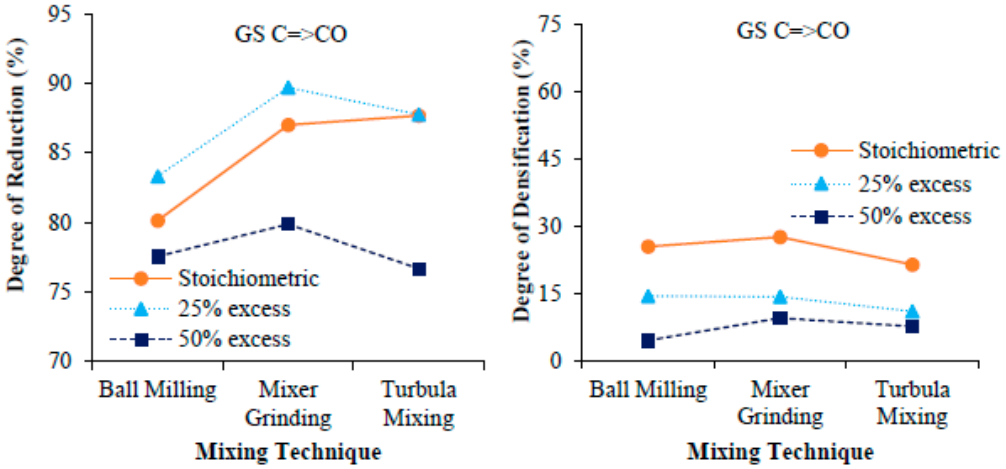

(b) Effect of interaction between Mixing Technique and Reducing agent addition on Degree of Reduction (DOR) and Degree of Densification (DOD) characteristics for the C => CO reduction mechanism

Figure 11. Effect of interaction of material parameters on DOR and DOD.

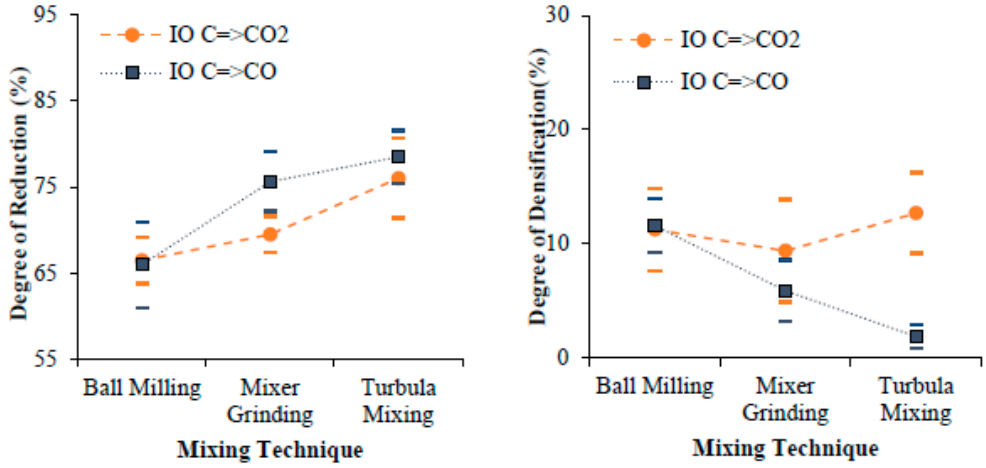

(a) Effect of Mixing Technique on Degree of Reduction (DOR) and Degree of Densification (DOD)

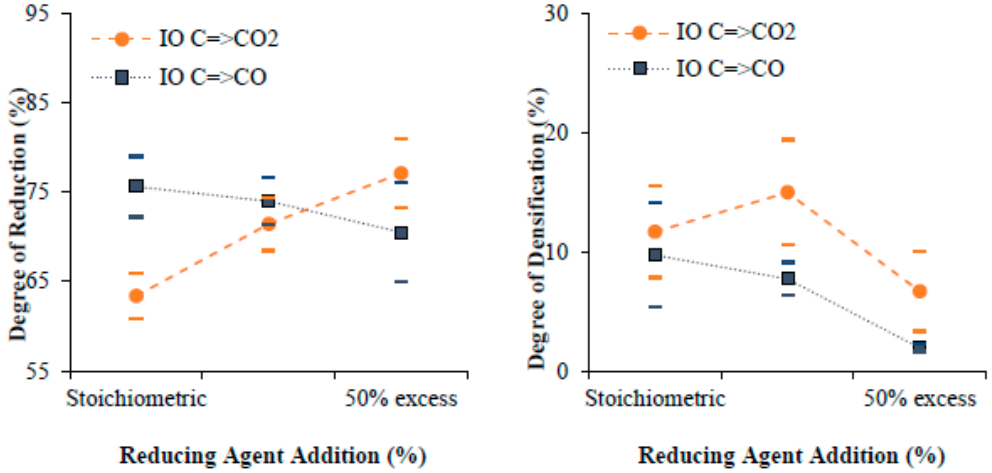

(b) Effect of addition of Reducing Agent on degree of reduction (DOR) and densification DOD

Figure 12. Main effects on the degree of reduction and degree of densification of iron ore of (**a**) mixing Technique and (**b**) addition of a reducing agent.

The flow of inert gas (Ar/N_2) during sintering also gave a higher degree of reduction (DOR) and degree of densification (DOD) for the study on reduction in iron ore (IO). Upon increasing the temperature of sintering, both the degree of reduction (DOR) and degree of densification (DOD) increased simultaneously, as is shown in Figure 13b. The levels of the reducing agent for facilitating a carbothermic reduction, the reduction in temperature, and the compaction pressure did not considerably change the two quality characteristics (i.e., degree of reduction (DOR) and degree of densification (DOD)). Either graphite or charcoal can be used for enabling carbothermic reduction of iron ore. A reduction in temperature to 100 °C below the sintering temperature, or to the same as the sintering temperature, is desirable for both the degree of reduction (DOR) and degree of densification (DOD). A compaction pressure of 1050 MPa was chosen for an overall improvement in the two quality characteristics (namely, DOR and DOD).

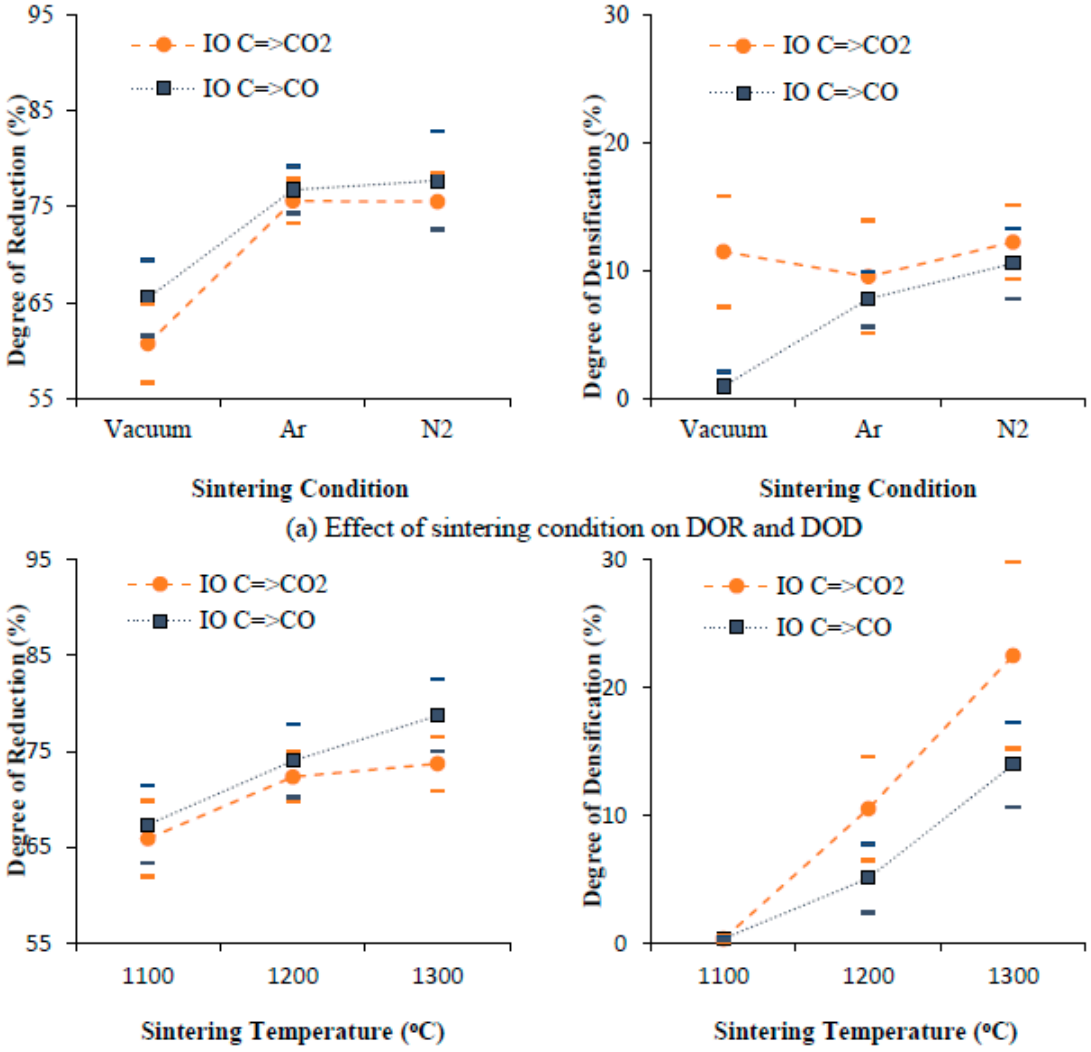

Figure 13. Main effects on the degree of reduction and densification of iron ore of (**a**) sintering condition and (**b**) sintering temperature.

5.2. Reduction Swelling Characteristics

The degree of reduction (DOR) and degree of densification (DOD) were both analyzed for parametric effect in the above section. A combination of use of a turbula mixer for mixing of the iron oxide with the reducing agent, a compaction pressure of 1050 MPa,

sintering in an environment of argon (Ar) gas, a reduction in temperature of 100 °C below the sintering temperature, and a sintering temperature of 1300 °C revealed the highest degree of reduction (DOR) and degree of densification (DOD). The observed characteristics for both of the considered and studied mechanisms did reveal the need for a reducing agent. Experimental observations did reveal that some of the pellets increased more in volume during reduction than the "green" pellets. This resulted in a low degree of densification (DOD). Similar observations were reported in earlier studies with specific reference to the reduction of pellets [22,27,32,33]. A quantification term for this behavior is the reduction swelling index (RSI). The RSI for each sample was calculated using the Expression (13):

$$\text{Reduction Swelling Index (RSI)} = \frac{V_f - V_i}{V_f} \quad (13)$$

where V_i is initial volume and V_f is the final volume of the pellet. The degree of reduction (DOR), degree of densification (DOD), and reduction swelling index (RSI) values of the four pellets samples corresponding to experimental conditions were then averaged to represent a single DOR, DOD and RSI for an experiment.

The degree of densification (DOD) and reduction swelling index (RSI) for the L27 experiments are plotted against the degree of reduction (DOR) and are shown in Figure 14. Both the degree of densification (DOD) and reduction swelling index (RSI) were not ordered systematically with an increase in the order of degree of reduction (DOR). This is because the parametric setting does tend to influence the degree of reduction (DOR) and degree of densification (DOD) differently. An increase in the degree of densification (DOD) and decrease in reduction swelling index (RSI) is roughly proportional to an increase in the degree of reduction (DOR).

The plots shown in Figure 14a have four distinct groups, with two each corresponding to (i) RSI versus DOR and (ii) DOD versus DOR for the two mechanisms considered. For samples of any mechanism studied, the reduction revealed a similar degree of reduction (DOR). Considering a combination of both direct reduction and indirect reduction [C=>CO=>CO_2], the addition of a reducing agent to the iron oxide seems to have an equal level of reduction completed when compared to that of samples having the reducing agent and with only direct reduction (C=>CO) being considered.

When considering the C=>CO=>CO_2 mechanism for the grinding-sludge (GS) powder, the pellets with a carbon addition (reducing agent) did reveal a higher degree of densification (DOD) for a near-similar degree of reduction (DOR) when compared to those that underwent the C=>CO mechanism. Similarly, the occurrence of swelling during reduction was higher for the pellets in which the reducing agents were added for the C=>CO mechanism. The excess carbon that was left behind following sintering and incomplete transformation to iron were the two key causes for an inferior degree of densification (DOD) characteristics of the chosen pellets. The plot for iron ore regarding (i) the degree of densification (DOD) versus the degree of reduction (DOR) and (ii) the reduction swelling index (RSI) versus the degree of reduction (DOR) (shown in Figure 14b), did not reveal a distinct trend for both degree of densification (DOD) and reduction swelling index (RSI) with increasing degree of reduction (DOR).

This confirms that the process of reduction is controlled by direct reduction as well as indirect reduction. The additional carbon added for the reduction of iron oxide is more than is required for the completion of the reduction process for the case of the C=>CO mechanism (Table 6). The carbon that is not utilized for reduction subsequently hinders the densification process. Most of the sintered samples of iron ore did reveal evidence of swelling. For these samples, the sintered density was lower than the "green" density. Thus, an operational mechanism for better recycling is C=>CO=>CO_2, in which the carbon (i.e., reducing agent) added for the purpose of reduction is used for both direct reduction and indirect reduction. The mechanism of C=>CO=>CO_2 is also useful for an overall improvement of densification since it provides reduced iron for densification and does not allow for the presence of reducing-agent residues following reduction.

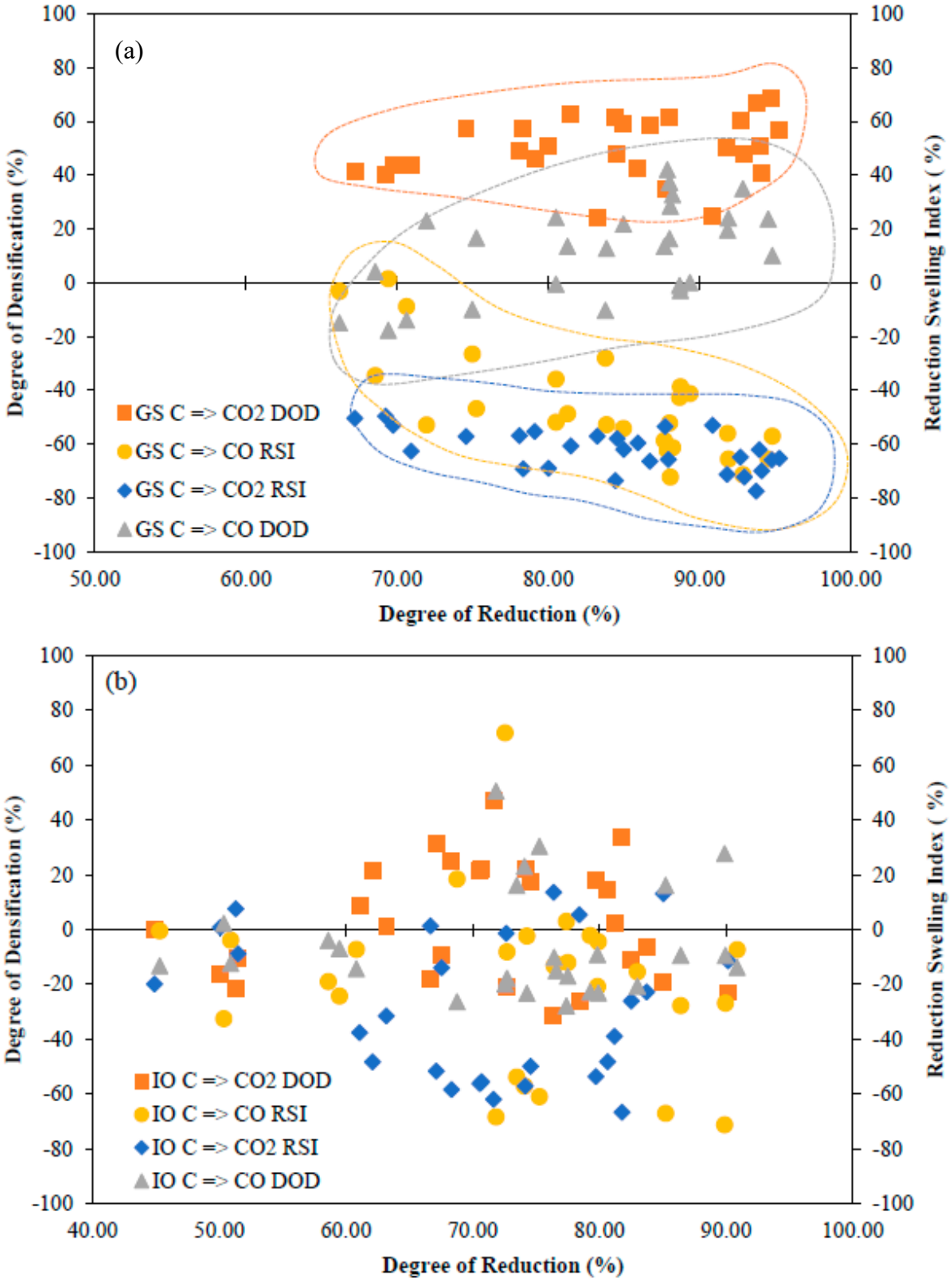

Figure 14. The effect of degree of reduction (DOR) on degree of densification (DOD) and reduction swelling index (RSI) for (**a**) grinding sludge (GS) and (**b**) iron ore (IO).

5.3. Discussion on Utility of Taguchi Method for Reduction and Densification

The reliability of the Taguchi-based experimental design and analysis approach used to study the reduction and densification characteristics was considered by predicting quality characteristics using the Taguchi addictive model. The addictive model, which

determines the effect of control parameters on S/N ratio of the experiment, is given by the Expression (14):

$$\eta_{\iota}\left(A_i,\ B_j, C_k, D_l,\ E_m,\ F_n,\ G_o\right) = \mu\ + a_i + \ b_j + c_k + d_l + e_m + f_n, + g_o + \epsilon \qquad (14)$$

The terms $a_{i,}$ b_j, c_k … g_o refer to deviation from the μ (mean) caused by the levels A_i, B_j, C_k … G_o of factors A, B, C … G, respectively, and ϵ = error.

The iron-oxide source and the reduction mechanism for the reliability test were chosen based on the best combination of the sources studied and the mechanism chosen. The additive model formula was used for the calculation of the two quality characteristics (i.e., the DOR and DOD) for the L27 matrix experimental setting and for the C=>CO=>CO_2 mechanism of reduction for the grinding sludge (GS). The predicted values of the degree of reduction (DOR) and degree of densification (DOD) were precision-calculated from the respective S/N ratio of the experiments (Expression (15)).

$$z_i\ = \sqrt{10^{(\eta_i/10)}} \qquad (15)$$

In this expression, z_i: represents the predicted value of quality characteristics (degree of reduction (DOR) and degree of densification (DOD)) for the i^{th} experiment among the L27 experimental array, η_i: S/N represents the ratio of the experiments, and i: is the experiment number.

The experimental and predicted values are much closer for the degree of reduction (DOR) than for the degree of densification (DOD) (Figure 15). However, both quality characteristics reveal an overall reliability of the Taguchi technique of experimentation. An analysis based on the Taguchi technique does give a robust solution/optimization for the present problem by eliminating the considered noise parameter coupled with best-setting among the levels of control parameters.

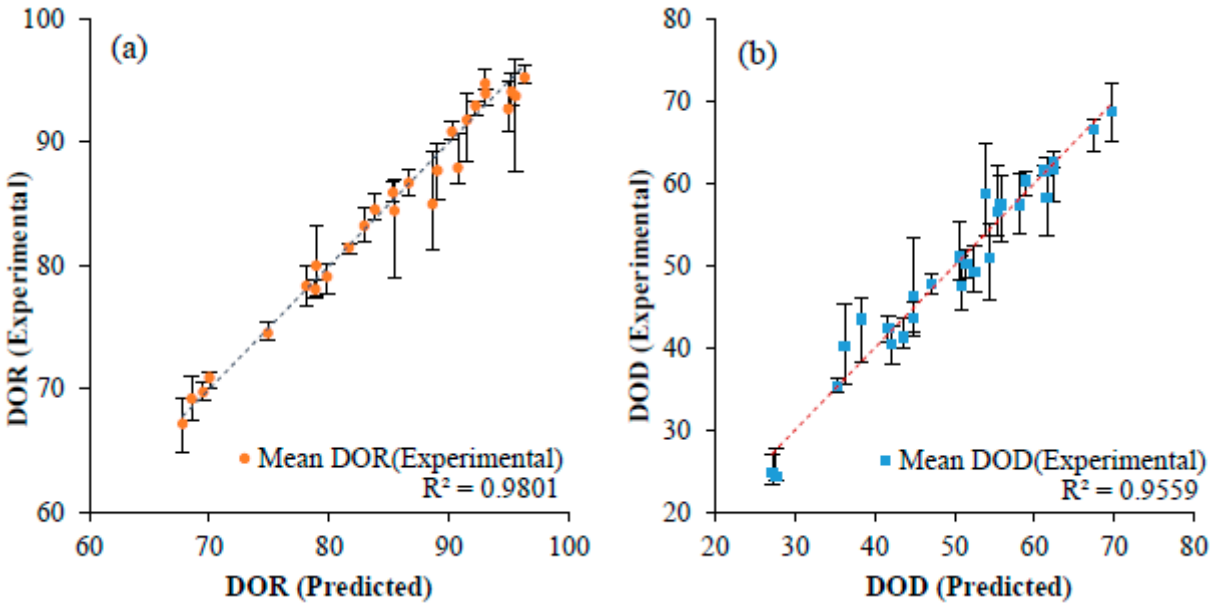

Figure 15. Comparison between experimental and predicted values of (**a**) degree of reduction (DOR) and (**b**) degree of densification (DOD) based on Taguchi experimental analysis.

6. Conclusions

The occurrence of in situ reduction and densification during the sintering step was confirmed through both experimental studies and empirical analysis. The key experimental outcomes from this study are the following:

1. The source of iron oxide shows distinct characteristics of sintered pellets. Grinding sludge as a source of oxide powder shows a higher degree of reduction (DOR) when compared one-on-one to a conventional oxide source (the iron ore used for the production of iron).
2. Graphite content in stoichiometric proportion gives the highest degree of densification, whereas an excess addition of graphite (between 25% in excess and 50% in excess) improves the degree of reduction (DOR) but creates a porous structure due to the formation and presence of excessive gaseous reaction products. Furthermore, an optimum graphite addition (25% in excess) helps to achieve the highest degree of reduction (DOR) and degree of densification (DOD).
3. An intermediate compaction pressure of 1050 MPa and a sintering temperature of 1200 °C were found to be the optimum levels for reducing and sintering (achieving highest degree of reduction and degree of densification) of cylindrically shaped components from scrap powder.
4. The degree of densification (DOD) is not significantly influenced by the degree of reduction (DOR) but is strongly influenced by the sintering parameters. The degree of reduction and the degree of densification (DOD) are higher for grinding sludge (GS) than for iron ore (IO) due to the presence of a higher quantity of unstable phases (Fe_3O_4) in the grinding sludge, which eases reduction.
5. The mixing technique, compaction pressure, and a variation in the reduction temperature with respect to sintering temperature was not found to be influential in improving the degree of densification (DOD) and degree of reduction (DOR) for any of the two mechanisms of reduction studied.
6. Carbon (particularly graphite) added to iron oxide and the C=>CO=>CO_2 mechanism is utilized fully through both direct reduction and indirect reduction. The degree of densification (DOD) for the C=>CO mechanism of reduction was noticeably lower in all the experimental runs due to the presence of excess residual carbon subsequent to sintering.

Author Contributions: Conceptualization, K.R. and P.D.; methodology, K.R.; software, K.R.; validation, K.R., P.D. and T.S.S.; formal analysis, K.R.; investigation, K.R.; resources, P.D.; data curation, K.R.; writing—original draft preparation, K.R.; writing—review and editing, T.S.S.; visualization, K.R.; supervision, P.D.; project administration, K.R.; funding acquisition, P.D. All authors have read and agreed to the published version of the manuscript.

Funding: This research received no external funding.

Conflicts of Interest: The authors declare no conflict of interest.

Appendix A

Table A1. Experimental conditions for L27 runs.

Exp. No.	A: Mixing Technique	B: Reducing Agent Addition (%)	C: Reduction Temperature (°C) below Sintering Temperature	D: Reducing Agent	E: Compaction Pressure (MPa)	F: Sintering Condition	G: Sintering Temp (°C)
1	Ball Milling	Stoic.	200	Graphite	900	Vacuum	1100
2	Ball Milling	Stoic.	100	Carbon Black	1050	Ar	1200
3	Ball Milling	Stoic.	0	Charcoal	1200	N_2	1300
4	Ball Milling	25% excess	200	Carbon Black	1050	N_2	1300
5	Ball Milling	25% excess	100	Charcoal	1200	Vacuum	1100
6	Ball Milling	25% excess	0	Graphite	900	Ar	1200
7	Ball Milling	50% excess	200	Charcoal	1200	Ar	1200
8	Ball Milling	50% excess	100	Graphite	900	N_2	1300

Table A1. *Cont.*

Exp. No.	A: Mixing Technique	B: Reducing Agent Addition (%)	C: Reduction Temperature (°C) below Sintering Temperature	D: Reducing Agent	E: Compaction Pressure (MPa)	F: Sintering Condition	G: Sintering Temp (°C)
9	Ball Milling	50% excess	0	Carbon Black	1050	Vacuum	1100
10	Mixer Grinding	Stoic.	200	Carbon Black	1200	Ar	1300
11	Mixer Grinding	Stoic.	100	Charcoal	900	N_2	1100
12	Mixer Grinding	Stoic.	0	Graphite	1050	Vacuum	1200
13	Mixer Grinding	25% excess	200	Charcoal	900	Vacuum	1200
14	Mixer Grinding	25% excess	100	Graphite	1050	Ar	1300
15	Mixer Grinding	25% excess	0	Carbon Black	1200	N_2	1100
16	Mixer Grinding	50% excess	200	Graphite	1050	N_2	1100
17	Mixer Grinding	50% excess	100	Carbon Black	1200	Vacuum	1200
18	Mixer Grinding	50% excess	0	Charcoal	900	Ar	1300
19	Turbula Mixing	Stoic.	200	Charcoal	1050	N_2	1200
20	Turbula Mixing	Stoic.	100	Graphite	1200	Vacuum	1300
21	Turbula Mixing	Stoic.	0	Carbon Black	900	Ar	1100
22	Turbula Mixing	25% excess	200	Graphite	1200	Ar	1100
23	Turbula Mixing	25% excess	100	Carbon Black	900	N_2	1200
24	Turbula Mixing	25% excess	0	Charcoal	1050	Vacuum	1300
25	Turbula Mixing	50% excess	200	Carbon Black	900	Vacuum	1300
26	Turbula Mixing	50% excess	100	Charcoal	1050	Ar	1100
27	Turbula Mixing	50% excess	0	Graphite	1200	N_2	1200

References

1. Rane, K.; Date, P. Reduction and densification characteristics of iron oxide metallic waste during solid state recycling. *Adv. Powder Technol.* **2015**, *26*, 126–138. [CrossRef]
2. Kumar, M.; Patel, S.K. Assessment of Reduction Behavior of Hematite Iron Ore Pellets in Coal Fines for Application In Sponge Ironmaking. *Miner. Process. Extr. Met. Rev.* **2009**, *30*, 240–259. [CrossRef]
3. Sastri, M.V.C.; Viswanath, R.P.; Viswanathan, B. Studies on the reduction of iron oxide with hydrogen. *Int. J. Hydrog. Energy* **1982**, *7*, 951–955. [CrossRef]
4. Cheng, G.-J.; Liu, J.-X.; Liu, Z.-G.; Chu, M.-S.; Xue, X.-X. Non-isothermal reduction mechanism and kinetics of high chromium vanadium–titanium magnetite pellets. *Ironmak. Steelmak.* **2015**, *42*, 17–26. [CrossRef]
5. Donskoi, E.; McElwain, D.L.S.; Wibberley, L.J. Estimation and modeling of parameters for direct reduction in iron ore/coal composites: Part II. Kinetic parameters. *Met. Mater. Trans. A* **2003**, *34*, 255–266. [CrossRef]
6. Bahgat, M.; Halim, K.S.A.; El-Kelesh, H.A.; Nasr, M.I. Enhancement of wüstite reducibility in blast furnace: Reaction kinetics and morphological changes. *Ironmak. Steelmak.* **2012**, *39*, 327–335. [CrossRef]
7. Bahgat, M.; Halim, K.S.A.; El-Kelesh, H.A.; Nasr, M.I. Behaviour of wüstite prepared from Baharia iron ore sinter during reduction with CO–CO2–N2gas mixture. *Miner. Process. Extr. Met.* **2011**, *120*, 102–110. [CrossRef]
8. Abdollahi, H.; Mahdavinejad, R.; Leavoli, R.P.; Ghambari, M.; Moradi, M. Investigation and optimization of properties of sintered iron/recycled grey cast iron powder metallurgy parts. *Proc. Inst. Mech. Eng. Part B J. Eng. Manuf.* **2014**, *229*, 1010–1020. [CrossRef]
9. Abdollahi, H.; Mahdavinejad, R.; Ghambari, M.; Moradi, M. Investigation of green properties of iron/jet-milled grey cast iron compacts by response surface method. *Proc. Inst. Mech. Eng. Part B J. Eng. Manuf.* **2014**, *228*, 493–503. [CrossRef]
10. Articles, T. Nakamura, Introduction of Grinding Swarf Recycling. *Ntn Tech. Rev.* **2004**, *71*, 80–83.
11. Fu, P.; Dai, X.; Zhang, Q.; Beijing, T. Recycling of Steel-making Dust and Preparation of Iron Oxide Red. 2014, 86, pp. 1–7. Available online: https://silo.tips/download/recycling-of-steel-making-dust-and-preparation-of-iron-oxide-red (accessed on 1 December 2022).
12. Materials, O. Iron Unit Recycling. 2001; 2000, pp. 1999–2000. Available online: https://www.energy.gov/sites/prod/files/2013/11/f4/roadmap_chap3.pdf (accessed on 1 December 2022).
13. Delavari, M.; Salarvand, A.; Rahi, A.; Shahri, F. The effect of powder metallurgy process parameters on mechanical properties of micro and nano-iron powder. *Int. J. Eng. Sci. Technol.* **2011**, *3*, 86–94. [CrossRef]
14. Komatina, M. The Sticking Problem During Direct Reduction of Fine Iron Ore In The Fluidized Bed Problem. 'Stikinga' Tokom Redukcije Rude Gvož Đ A, Malih Dimenzija Č Estica U Fluidizovanom Sloju. *Metall. Mater. Eng.* **2004**.

15. Emamian, A. A Study on Wear Resistance, Hardness and Impact Behaviour of Carburized Fe-Based Powder Metallurgy Parts for Automotive Applications. *Mater. Sci. Appl.* **2012**, *3*, 519–522. [CrossRef]
16. Nerjavnega, L.; Nega, O.; Mim-tehnologijo, I.Z.; Butkovi, S.; Oru, M.; Mehmedovi, M. Effect Of Sintering Parameters On The Density, Microstructure And Mechanical Properties Of The Niobium-Modified Heat-Resistant Stainless Steel Gx40crnisi25-20 Produced By Mim Technology. *Mater. Tehnol.* **2012**, *46*, 185–190.
17. Mashhadi, H.A.; Rastgoo, A.; Khaki, J.V. An Investigation on the Reduction of Iron Ore Pellets in Fixed Bed of Domestic Non-Coking Coals. *Int. J. ISSI* **2008**, *5*, 8–14.
18. Manchili, S.K.; Wendel, J.; Hryha, E.; Nyborg, L. Analysis of iron oxide reduction kinetics in the nanometric scale using hydrogen. *Nanomaterials* **2020**, *10*, 1276. [CrossRef] [PubMed]
19. Sintered Iron-Based Materials Chapter 9. Available online: https://mail.pk.edu.pl/~{}mnykiel/iim/26/DOWNLOAD/pdf/CHAPT09.PDF (accessed on 1 December 2022).
20. Dewidar, M. Influence of processing parameters and sintering atmosphere on the mechanical properties and microstructure of porous 316L stainless steel f or possible hard-tissue applications. *Int. J. Mech. Mech. Eng.* **2012**, *12*, 10–24.
21. El-Geassy, A.A.; Halim, K.S.A.; Bahgat, M.; Mousa, E.A.; El-Shereafy, E.E.; El-Tawil, A.A. Carbothermic reduction of Fe_2O_3/C compacts: Comparative approach to kinetics and mechanism. *Ironmak. Steelmak.* **2013**, *40*, 534–544. [CrossRef]
22. Donskoi, E.; McElwain, D.L.S.; Wibberley, L.J. Sensitivity analysis of a model for direct reduction in swelling coal char-hematite composite pellets. *ANZIAM J.* **2003**, *44*, 140–159. [CrossRef]
23. Bahgat, M.; Halim, K.S.A.; Nasr, M.I. Effect of Nature Gas Injection on Reducibility of Wustite Prepared from Baharia Iron Ore Sinter. *J. Metall. Eng.* **2012**, *1*, 14–22.
24. Xu, B.; Hou, T.; Chen, X.-L.; Li, Q.; Jiang, T.; Li, P. Effect of dolomite on reduction swelling property of iron ore pellets. *J. Central South Univ.* **2013**, *20*, 2806–2810. [CrossRef]
25. Rane, K.K.; Date, P.P. Sustainable Recycling of Ferrous Metallic Scrap Using Powder Metallurgy Process. *J. Sustain. Met.* **2017**, *3*, 251–264. [CrossRef]
26. Rane, K.; Date, P.P. Recycling Potential for Finely Divided Ferrous Metallic Scrap Using Powder Technology. *Recycling* **2018**, *3*, 59. [CrossRef]
27. Nascimento, R.; Mourão, M.; Capocchi, J. Kinetics and catastrophic swelling during reduction of iron ore in carbon bearing pellets. *Ironmak. Steelmak.* **1999**, *26*, 182–186. [CrossRef]
28. Heikkilä, A.; Iljana, M.; Bartusch, H.; Fabritius, T. Reduction of iron ore pellets, sinter, and lump ore under simulated blast furnace conditions. *Steel Res. Int.* **2020**, *91*, 2000047. [CrossRef]
29. Al-tounsi, A.; Ireland, H. Effect of sintering parameters on the mechanical and physical properties of sinter formed materials. 1992. Available online: https://doras.dcu.ie/18312/.
30. Çavdar, U.; Sad, B.; At, E. Effect of The Copper Amount In Iron-Based Powder-Metal Compacts. Vpliv Vsebnosti Bakra V Kovinskih Stisnjencih Iz. *Mater. Tehnol.* **2015**, *49*, 57–62.
31. Philips, T.; Dwyer, J.J.; Zurecki, Z. *Controlling Properties of Sintered Steel Powder Metal Components Using Atmosphere Composition as a Variable*; Air Products and Chemicals Inc.: Allentown, PA, USA, 2006.
32. Yi, L.; Huang, Z.; Jiang, T.; Wang, L.; Qi, T. Swelling behavior of iron ore pellet reduced by H2–CO mixtures. *Powder Technol.* **2015**, *269*, 290–295. [CrossRef]
33. Iljana, M.; Mattila, O.; Alatarvas, T.; Visuri, V.V.; Kurikkala, J.; Paananen, T.; Fabritius, T. Dynamic and isothermal reduction swelling behaviour of olivine and acid iron ore pellets under simulated blast furnace shaft conditions. *ISIJ Int.* **2020**, *52*, 1257–1265. [CrossRef]